Aiyuan Ma, Xuemei Zheng, Shixing Wang, Jinhui Peng*, Libo Zhang* and Zhiqiang Li

Study on dechlorination kinetics from zinc oxide dust by clean metallurgy technology

DOI 10.1515/gps-2015-0041
Received June 2, 2015; accepted August 17, 2015; previously published online January 12, 2016

Abstract: Cavity perturbation method was used to determine the dielectric properties (ε', ε'', and tan δ) of zinc oxide dust. The process of dechlorination from zinc oxide dust by microwave roasting was evaluated considering the effect of different roasting temperatures and holding times. The research results showed that the $ZnCl_2$ and $PbCl_2$ with high-loss factor were heated preferentially by microwave, and the dechlorination rate can reach 97.22% after microwave roasting at 650°C for 40 min. The phases of zinc oxide dust before and after microwave roasting were observed and characterized by X-ray diffraction (XRD) analysis. The kinetics of dechlorination from zinc oxide dust was investigated. The three kinetic factors were obtained by the dynamic isothermal method, which provided a theoretical basis for dechlorination from zinc oxide dust. Thermodynamic analysis showed that the volatilization of chlorides was mainly ionic crystal phase transition process. The volatile kinetics of zinc oxide dust were controlled by the solid state diffusion and interface chemical reaction, during the microwave heating, with an activation energy E=46.6 KJ/mol and the reaction order n is level 1.

Keywords: dechlorination; dielectric property; kinetics; microwave roasting; zinc oxide dust.

***Corresponding authors: Jinhui Peng and Libo Zhang,** Yunnan Provincial Key Laboratory of Intensification Metallurgy, Kunming 650093, China; National Local Joint Laboratory of Engineering Application of Microwave Energy and Equipment Technology, Kunming, Yunnan 650093, China; Key Laboratory of Unconventional Metallurgy, Ministry of Education, Kunming 650093, China; and Faculty of Metallurgical and Energy Engineering, Kunming University of Science and Technology, Kunming 650093, China, e-mail: jhpeng@kmust.edu.cn (J. Peng); libozhang77@163.com (L. Zhang)
Aiyuan Ma, Xuemei Zheng, Shixing Wang and Zhiqiang Li: Yunnan Provincial Key Laboratory of Intensification Metallurgy, Kunming 650093, China; National Local Joint Laboratory of Engineering Application of Microwave Energy and Equipment Technology, Kunming, Yunnan 650093, China; Key Laboratory of Unconventional Metallurgy, Ministry of Education, Kunming 650093, China; and Faculty of Metallurgical and Energy Engineering, Kunming University of Science and Technology, Kunming 650093, China

1 Introduction

With the depletion of zinc concentrate due to the continuous development and utilization of resources, zinc oxide dust and other secondary resource utilizations are an effective means to alleviate the shortage of raw materials for zinc and lead companies [1–4]. However, chlorine in zinc oxide dust will cause aluminum cathode and anode grid corrosion, corrosion of equipment and reduce power quality zinc, in addition to causing other serious harm to the subsequent zinc electro-winning process [5, 6]. Chlorine in zinc oxide dust must be removed. Cl ion concentrations in electrolytes must meet electrolysis requirements (F<80 mg/l, Cl<100 mg/l) in the zinc electrolysis process [7, 8]. According to the lower boiling point of chlorides and volatility at high temperature, the most common dechlorination methods, such as roasting approaches of multiple hearth furnaces and rotary kilns, are commercially being adopted to remove Cl from leach liquor. The zinc oxide dust was roasted under a certain negative pressure for the occurrence of physical and chemical reactions, so that the low boiling point chlorides volatilize into the gas phase. The removal efficiency from high chloride concentrations using roasting approaches is low. The methods have problems of high temperature, high energy consumption, and so on [9–12].

Microwave metallurgy as an efficient, clean metallurgical technology is widely used in drying, assisted grinding, assisted reduction and strengthening leaching [13–17]. The material with high-loss factor is heated preferentially by microwave, and a phase interface is created with a large temperature gradient. Phase interface cracks are generated, which strengthen phase separation [18]. Based on the advantage of microwave selective heating, the valuable lead and zinc chloride evaporation can be strengthened to achieve dechlorination purposes. Dechlorination of zinc oxide dust by microwave roasting is an efficient method [19, 20].

Dielectric properties are defined in terms of complex permittivity (ε), composed of a real part (ε' dielectric constant) and an imaginary part (ε'' dielectric loss factor) by the equation: $\varepsilon=\varepsilon'-j\varepsilon''$. Loss tangent (tan δ), a parameter used to describe how well a material absorbs microwave energy, is the ratio of dielectric loss factor and the dielectric

constant (tan $\delta=\varepsilon''/\varepsilon'$) [21]. A material with a higher loss tangent will heat faster under a microwave field as compared to a material with a lower loss tangent [22].

The main dynamics of dechlorination of zinc oxide dust by microwave roasting is the objective of the present work. The microwave roasting technique could effectively remove harmful impurities from zinc oxide dust, and create the best dynamic conditions. The authors provide direct and theoretical support for the dechlorination from zinc oxide dust by microwave roasting, promoting further improvement and progress in the zinc smelting process.

2 Materials and methods

2.1 Experimental materials

The zinc oxide dust used in the experiments was received from a Pb and Zn smelting enterprise, in Yunnan Province in China. The particle size distribution of zinc oxide dust was analyzed by a Rise-2002 laser particle size analyzer (Jinan Rise Science & Technology Co., Ltd., China) and the results showed that the average particle size of D_{av}=1.01 μm; 99.87% of dust is below 3 μm in particle size. The sample composition was characterized by X-ray diffraction (Rigaku Company, Japan) and X-ray fluorescence (ARL 9900, Thermo Fisher Scientific, Switzerland) measurements. Scanning electron microscopy (XL30ESEM-TMP, Philips Company, Holland) equipped energy dispersive spectroscopy (GENESIS, EDAX Company, USA) was used for analyzing the morphology and microscopic chemical composition of the zinc oxide dust.

The main chemical composition of the zinc oxide dust is listed in Table 1, which reveals that the lead and zinc content are 15.94% and 67.22%, respectively, and the chlorine content is 3.08%. The XRD spectrum of the zinc oxide dust is displayed in Figure 1, which shows that the samples used in this work were mainly composed of ZnO, $PbSO_4$ and chlorine containing compounds ($ZnCl_2$ and $PbCl_2$).

The microstructure of the zinc oxide dust is shown in Figure 2, which shows that two different phases with various microstructures exist in the zinc oxide dust, namely, the amorphous structure (a) and the spherical structure (b). To obtain more information of the elements distribution characteristics in the zinc oxide dust, especially that of Cl, X-ray EDS line scanning of the elements distribution characteristics in the spherical and amorphous structure was performed, as shown in Figure 3. The EDS line scanning shows that the distribution characteristics of Zn and O elements are the same in the spherical phase, and the Pb, Zn, S, Cl and O elements are rich in the amorphous structure. Combined with the XRD analysis results as shown in Figure 1, the phase in the spherical structure is ZnO, and the amorphous structure might be composed of the mixtures of $ZnCl_2$, $PbCl_2$ and $PbSO_4$.

Table 1: The chemical compositions of zinc oxide dust (mass fraction, %).

Element	Zn	Pb	Fe	Si	Ca	S	Cl	In
Weight (mass %)	67.22	15.94	3.02	0.72	0.61	2.46	3.08	0.14

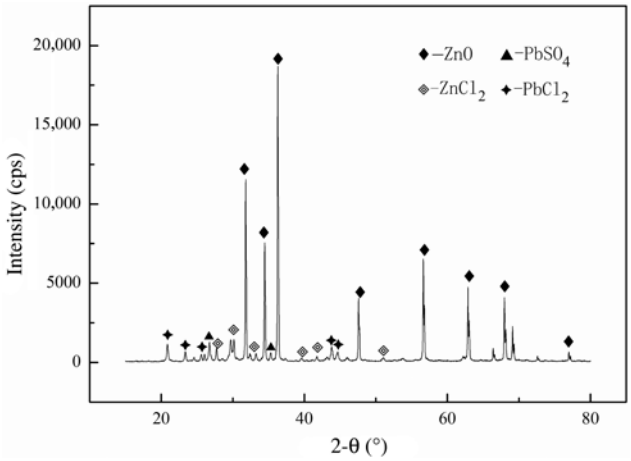

Figure 1: X-ray diffraction pattern of zinc oxide dust sample.

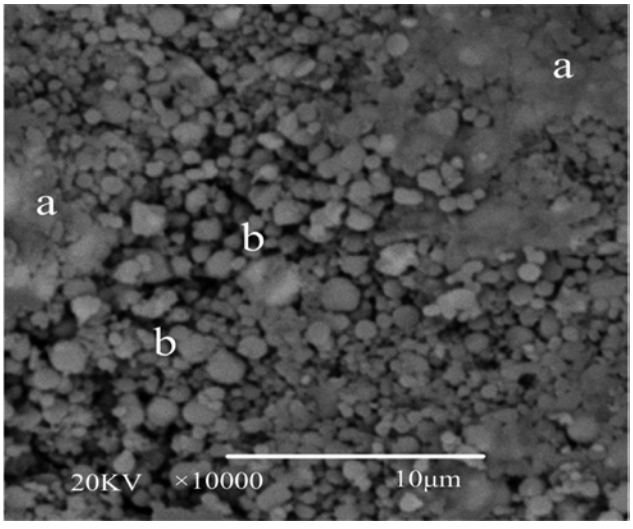

Figure 2: Scanning electron micrographs of zinc oxide dust particles.

2.2 Experimental set-up and methods

2.2.1 Test device for dielectric parameters: The dielectric parameters measuring device scheme is shown in Figure 4. The dielectric parameter tester (Dielectric kit for Vials) is supplied by a German Püschner company. The device consists of a microwave power source, a directional coupler, a microwave receiver and a cavity resonator. The microwave signal receiver of the AD-8320 integrated circuit can detect the signal amplitude and phase. The resonator was used to hold in the analyzing cavity. The test control unit is via a USB data cable connected to the computer that calculates the dielectric parameters. The system error of the dielectric coefficient real parts was estimated to be 1–2% during the perturbation method tests. Deionized water (the real part of permittivity is 80.4 F/m) [23] was used and polytetrafluoroethylene (the real part of permittivity is 2.08 F/m) [24] was the standard resulting in 76.79 F/m and 2.04 F/m, respectively, 4.49 and 1.92% differences. During the measuring experiment, powders or liquids are mixed and filled into the vial.

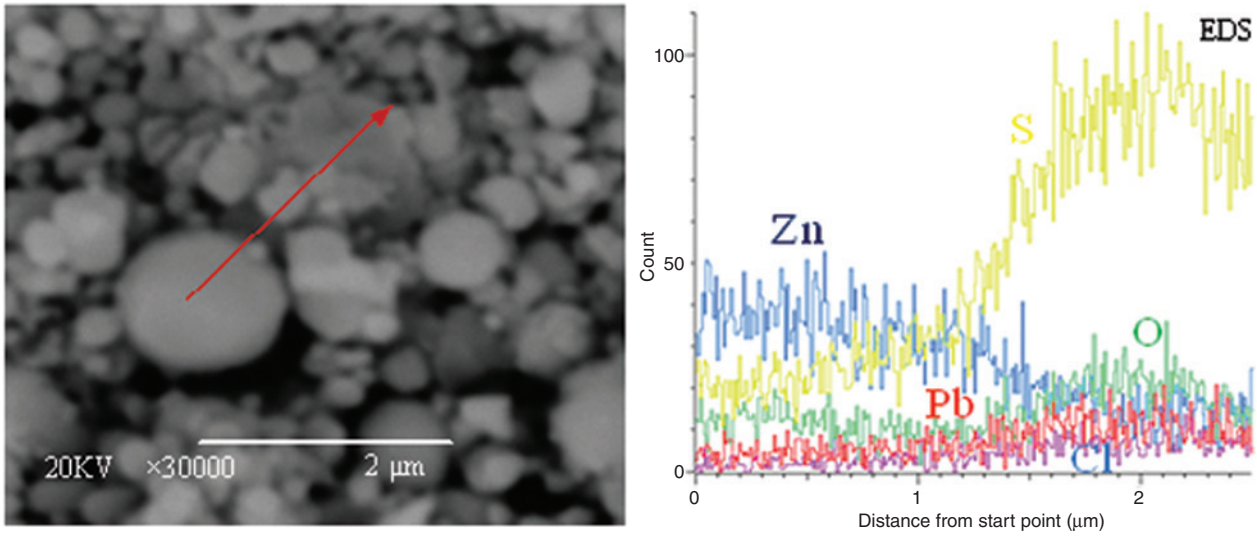

Figure 3: Energy dispersive spectroscopy (EDS) line scanning results of zinc oxide dust sample (red line).

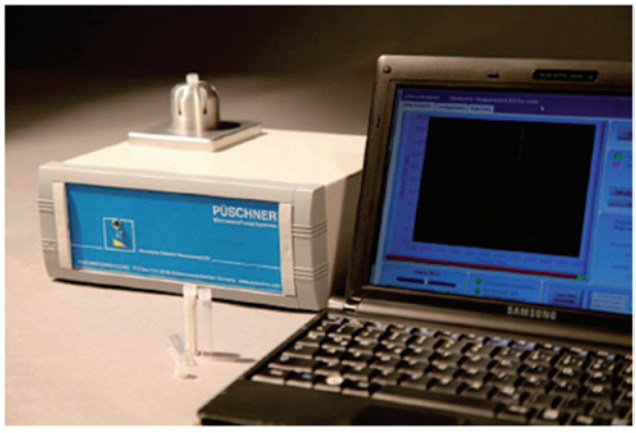

Figure 4: Zinc oxide dust dielectric constant measurement device scheme.

2.2.2 Microwave roasting equipment: A 3-kW box-type microwave reactor developed by the Key Laboratory of Unconventional Metallurgy in the Ministry of Education of Kunming University of Science and Technology was utilized for experimentation. The experimental set up is shown in Figure 5.

The microwave heating frequency is 2450 MHz, while the power can be varied from 0 kW to 3 kW. A K type thermocouple with shielded sleeves was used to measure the temperature. A mullite crucible with an inner diameter of 90 mm, height of 120 mm, with good wave-transparent and heat shock properties was used as the material support. The device was equipped with a mixing system, with an rpm of 0–120, to facilitate intense mixing of the zinc oxide dust. A dust absorption system was developed to collect the flue dust generated in the experimental process. This system is comprised of a dust collection bottle, a water-absorption bottle, an alkali-absorption bottle, a buffer bottle and a miniature pump.

2.2.3 Experimental methods: Zinc oxide dust (300 g) was accurately quantified and placed in a microwave reactor box. The effects of roasting temperatures (550°C, 600°C, 650°C) and holding times (10 min, 20 min, 40 min, 60 min) on the dechlorination were studied, and the other constant parameters of the microwave roasting experiments were as follows: air flow rate of 300 l/h and stirring speed of 60 rpm. The silver chloride turbidimetric method was used for analyzing the chlorine content in the samples before and after microwave roasting [25].

3 Results and discussion

3.1 Dielectric property test results and analysis

The dielectric constant (ε') is a measure of the ability of the dielectrics to store electrical energy, while the dielectric loss (ε'') represents the loss of electrical energy in dielectrics. The energy lost from the electric field to the dielectric is eventually converted into thermal energy or heat. Thus, for dielectrics with no magnetic properties, the imaginary part of complex relative permittivity determines the heating rate when microwave energy is applied [26].

The dielectric parameters (ε', ε'' and tan δ) of zinc oxide dust, ZnO, $ZnCl_2$, PbO and $PbCl_2$ were measured at room temperature at 2.45 GHz by the cavity perturbation method, and the results are presented in Table 2.

As the results show in Table 2, the loss factor of zinc chloride and lead chloride are 0.0837 and 0.0374, which are higher than that of zinc oxide (0.0357) and lead oxide (0.0098), respectively. In addition, the dielectric loss of zinc oxide dust (0.13) is higher than any kind of substances. The material with high-loss factor is heated preferentially

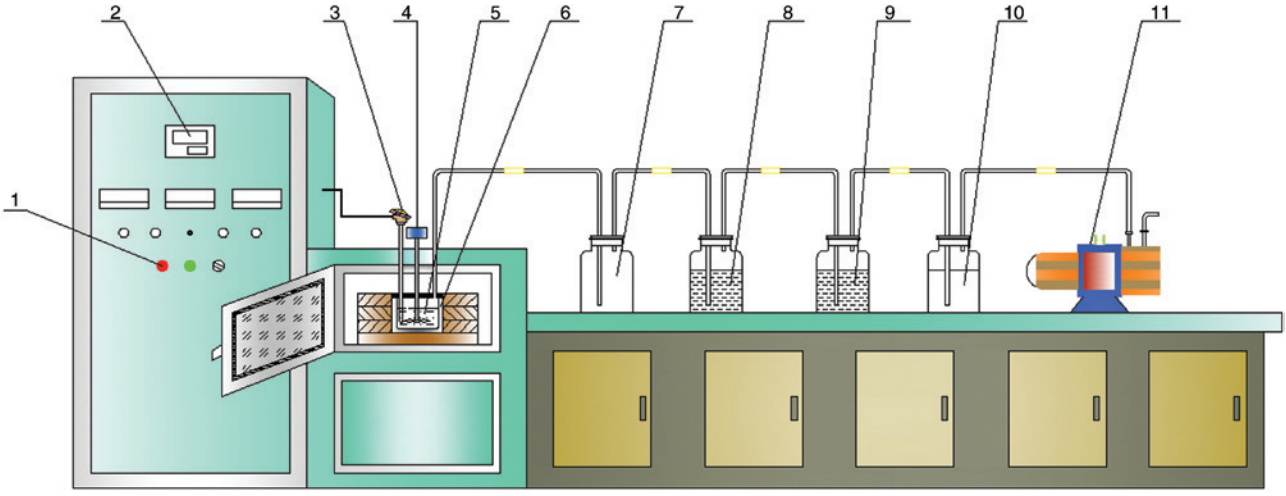

Figure 5: Experiment equipment for microwave roasting. 1-the control system of microwave; 2-temperature display; 3-thermocouple; 4-blender; 5-zinc oxide dust sample; 6-mullite crucible; 7-dust collection bottle; 8-a water-absorption bottle; 9-alkali-absorption bottle; 10-buffer bottle; 11-miniature pump.

Table 2: Dielectric parameters of different substances.

Parameters / Substances	Dielectric constant ε' (F/m)	Loss factor ε'' (F/m)	Loss tangent $\tan\delta$
ZnO	1.4031	0.0357	0.0254
$ZnCl_2$	2.0276	0.0837	0.0413
PbO	2.4291	0.0098	0.0040
$PbCl_2$	4.7428	0.0374	0.0079
Zinc oxide dust	3.14	0.13	0.0414

by microwave, and a phase interface is created with a large temperature gradient. Phase interface cracks are generated, which strengthen phase separation. Research shows that the microwave absorbance ability of chloride is strong, while that of Zn and Pb oxide is weak in the zinc oxide dust. Hence, utilizing the selective heating property of microwaves, the separation of impurities (chloride) as volatile components can be strengthened meeting the electrolysis process requirements.

3.2 Thermodynamic analysis of chloride

Under the air atmosphere, there is the presence of O_2 and H_2O. Zinc chloride and lead chloride are crystals under high temperature conditions, and the reactions of chloride volatilization are phase transformation including physical and chemical reactions of O_2 and H_2O [27–29].

$ZnCl_2$ chemical reactions may occur as follows:

$$ZnCl_2(s)+1/2O_2(g)=ZnO(s)+Cl_2(g) \quad (1)$$

$$ZnCl_2(s)+H_2O(g)=ZnO(s)+2HCl(g) \quad (2)$$

The variation curve of Gibbs free energy with the change of temperature is shown in Figure 6.

As can be seen from Figure 6, the Gibbs free energy changes of Eqs. (1) and (2) in the 25°C~732°C range are over zero ($\Delta G>0$) under air atmosphere. Eqs. (1) and (2) cannot occur. The changes of Gibbs free energy with temperature as displayed in Eqs. (1) and (2) show that volatile $ZnCl_2$ cause the phase transformation, as a result $ZnCl_2$ transformated to ZnO in air mainly at the high temperature (>732°C).

$PbCl_2$ may combine with O_2 and H_2O under a high temperature atmosphere [30, 31]. The reactions are follows:

$$PbCl_2(s)+H_2O(g)=PbO(s)+2HCl(g) \quad (3)$$

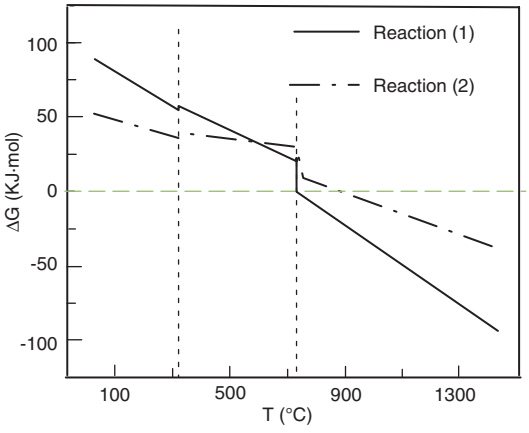

Figure 6: Relationship between ΔG of $ZnCl_2$ volatile reaction and temperature.

$$PbCl_2(s)+H_2O(g)=PbO(g)+2HCl(g) \quad (4)$$

$$PbCl_2(s)+1/2O_2(g)=PbO(s)+Cl_2(g) \quad (5)$$

$$PbCl_2(s)+1/2O_2(g)=PbO(g)+Cl_2(g) \quad (6)$$

$$PbCl_2(s)+1/4O_2(g)=1/2PbO(s)+1/2PbCl_4(g) \quad (7)$$

$$PbCl_2(s)+1/4O_2(g)=1/2PbO(g)+1/2PbCl_4(g) \quad (8)$$

The Gibbs free energy changes of Eqs. (3)–(8) with temperature are shown in Figure 7. These reactions probably occur under high temperature, which means that the volatilization of $PbCl_2$ is mainly a phase change to gas and the transformation process of $PbCl_2$ to PbO in air atmosphere at a high temperature. In addition, according to the melting point, boiling point and vapor pressure of zinc oxide dust which are presented in Table 3, it can be observed that the melting point and the boiling point of $ZnCl_2$ and $PbCl_2$ were low. The volatile reaction of metal halide under high temperature is the process of gaseous halide ionic crystals and solid phase diffusion from escaping.

Based on the above thermodynamic analysis of zinc oxide dust (Figures 6 and 7), we found that $ZnCl_2$ and $PbCl_2$ cannot react with O_2 and H_2O at low temperatures

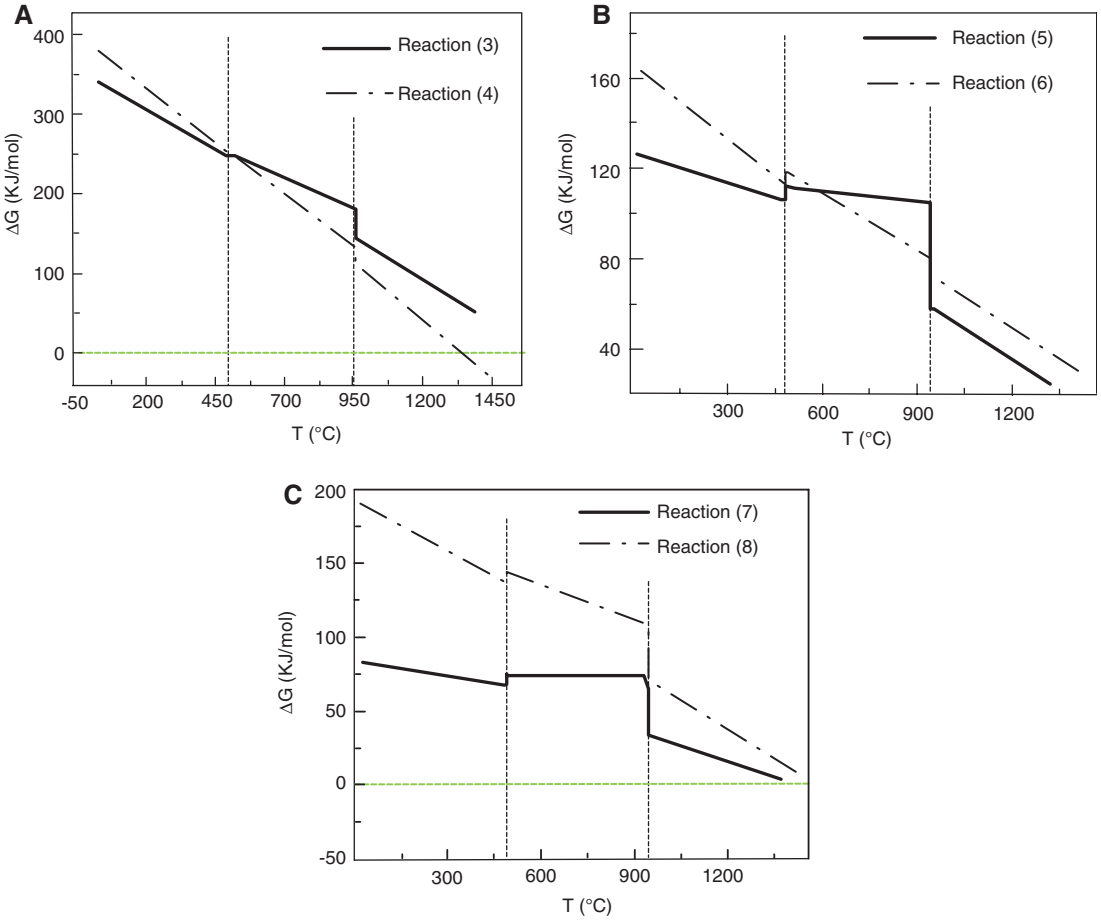

Figure 7: The relationship between ΔG of $PbCl_2$ reaction and temperature: (A) Eqs. (3) and (4), (B) Eqs. (5) and (6), (C) Eqs. (7) and (8).

Table 3: The melting point, boiling point and vapor pressure of zinc oxide dust [32].

Compounds	Melting point (°C)	Boiling point (°C)	Vapor pressure (Pa)				
			550°C	650°C	750°C	850°C	950°C
$ZnCl_2$	365	732	4.38×10^3	3.15×10^4	1.46×10^5	4.93×10^5	1.32×10^6
$PbCl_2$	501	952	1.54×10^2	1.49×10^3	8.59×10^3	3.43×10^4	1.01×10^5

(<732°C). However, phase transformation of $ZnCl_2$ and $PbCl_2$ occurred from solid phase to gas phase at the range of 500~732°C. Combined with the fact that the melting point of ZnO is 1970°C and that of PbO is 888°C, the experimental temperatures were finally determined at a range of 550~650°C for the sake of the separation of $ZnCl_2$ ($PbCl_2$) and ZnO (PbO). In addition, we strengthened the quick volatilization of $ZnCl_2$ and $PbCl_2$ by blowing air through in the course of the roasting experiment.

3.3 Kinetic experiments of dechlorination

3.3.1 Effects of temperature on dechlorination rate

Figure 8 presents the effect of temperature on the dechlorination rates of the zinc oxide dust in the range of 550~650°C. The results indicate that 40 min are required for the complete removing of the chloride, and the dechlorination rate can reach 97.22% at 650°C. The temperature strongly influences the dechlorination rate, which increased from 86.19% at 550°C to 97.22% at 650°C.

The XRD patterns of the samples before and after microwave roasting at 650°C are shown in Figure 9. Obviously, the peaks for $ZnCl_2$ and $PbCl_2$ diminished significantly in the roasted sample, which means the chlorine containing compounds ($ZnCl_2$ and $PbCl_2$) disappeared.

Compared with the traditional dechlorination process, the non-conventional process of microwave roasting for dechlorination from zinc oxide dust is more simple, clean and pollution-free, and the chlorine content in leaching solution met the requirements of the zinc electrolysis process. Table 4 shows the control conditions and comparisons of several dechlorination processes [6, 20, 33].

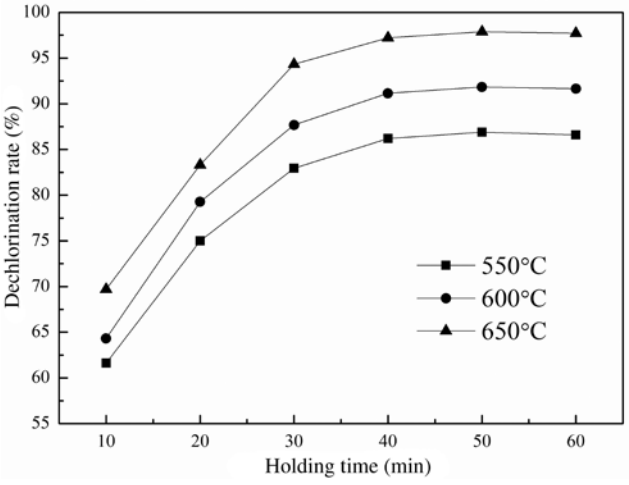

Figure 8: Effects of temperature on dechlorination rate.

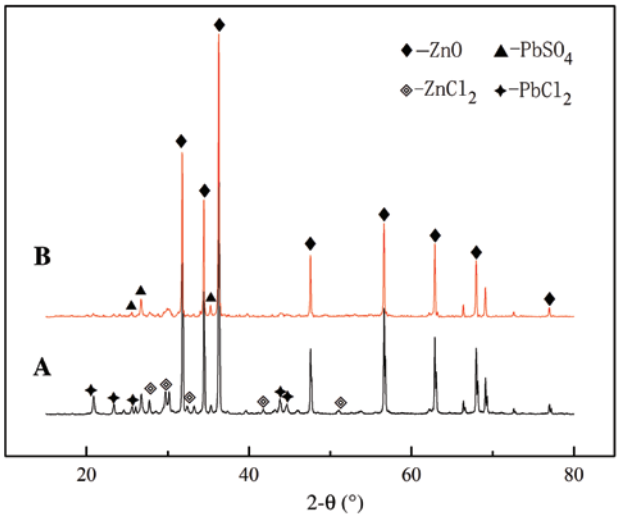

Figure 9: X-ray diffraction (XRD) patterns of zinc oxide dust before and after microwave roasting. (A) raw material, (B) the sample of roasting temperature at 650°C.

3.3.2 Kinetic analysis

The experimental program was setup to study the volatile kinetics of zinc oxide dust at different microwave roasting temperatures. The kinetics study of dechlorination belongs to a heterogeneous and homoisothermal reaction. The Arrhenius equation was introduced to investigate the kinetics of dechlorination from zinc oxide dust by microwave roasting. The apparent activation energies (E) were calculated using the Arrhenius equation [34, 35], and the Arrhenius equation is expressed as follows:

$$K = Ae^{-E/RT} \tag{9}$$

where A is the frequency factor or pre-exponential factor (s^{-1}), E is the activation energy (KJ/mol), R is the universal gas constant (R=8.314 J/[mol.k]) and T is the absolute temperature (K).

The Cl evaporation rate can be expressed as follows:

$$d\alpha / dt = Ae^{-E/RT} f(\alpha) = Ae^{-E/RT}(1-\alpha)^n \tag{10}$$

where α, n and t represent the dechlorination rate, the reaction order and the holding time, respectively.

According to Eq. (10), we introduced the kinetic mechanism function $G(\alpha)$, which is the integral form [Eq. (10)], as shown in Eq. (11):

$$G(\alpha) = \int_0^t Ae^{(-E/RT)} dt = Kt \tag{11}$$

According to Eq. (11), as reaction orders n are 0, 1/2, 2/3, 1 and 2, the relationship of reaction conversion percentage and holding time at 650°C can be easily obtained

Table 4: The control conditions and comparisons of several dechlorination processes.

Process	Temperature (°C)	Time (h)	Advantages and disadvantages
Roasting by multiple hearth furnaces	600~1000	1.5~4	(1) The ripest method (2) Huge equipment; high investment; high energy consumption; high cost of the center shaft damage repairment
Water washing, Caustic washing	80~95	2~4	(1) Easy manipulation; low cost (2) Large consumption of $NaCO_3$ caustic $NaSO_4$ and vapor (3) Produces large amount of waste water; the liquid after water washing or caustic washing must be processed appropriately to achieve the plant emission requirements; the need for a large number of water and sulfuric acid
Microwave roasting	550~750	0.3~1.0	Clean and non-pollution, low energy consumption, heating–selectivity, short reaction time and easy operation

by using the experimental data, and the $G(\alpha)$ and time curves are shown in Figure 10. The fitting results of the kinetic mechanism function $G(\alpha)$ and time are shown in Table 5.

After the data fitting to the experimental findings is carried on, it can be found that the best linearity is up to 0.988 (n=1), which indicates the feasibility and validity of the volatile dynamics of the reaction model. At the same time, the rate constant ($K_{650°C}$) is 0.0824 at 650°C.

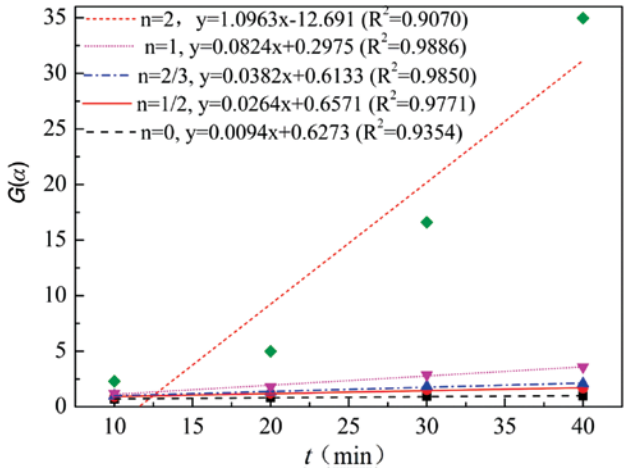

Figure 10: The relationship between $G(\alpha)$ and time at 650°C on n=0, 1/2, 2/3, 1, 2, respectively.

Table 5: The relationship between mechanism function and time at 650°C.

Reaction order	Fitting line	R^2
0	y=0.0094x+0.6273	0.9354
1/2	y=0.0264x+0.6571	0.9771
2/3	y=0.0038x+0.6133	0.985
1	y=0.0824x+0.2975	0.988
2	y=1.0963x-12.691	0.907

Similarly, it can be found that the best linearity of $G(\alpha)$ and time are up to 0.9959 (n=1) and 0.9987 (n=1) at 600°C and 550°C, respectively. The $G(\alpha)$ and time (t) curves are shown in Figures 11 and 12. The fitting results of the kinetic mechanism function $G(\alpha)$ and time are shown in Tables 6 and 7. Select the fittest mechanism function, the values of K at 600°C and 500°C are 0.0562 ($K_{600°C}$) and 0.0392 ($K_{550°C}$), respectively.

The modified logistic Arrhenius equation Eq. (9) was given in Eq. (12):

$$\ln K = \ln A - E / RT \tag{12}$$

In the calculated rate constants under different temperatures (550°C, 600°C, 650°C), a slope of regression line ($-E/RT$) was obtained through the use of ln K on the thermodynamic temperature of the reciprocal (T^{-1}) plot, and the data are presented in Table 8. The activation energy (E) was obtained through the slope of regression line, and A was obtained through the interception of the regression line.

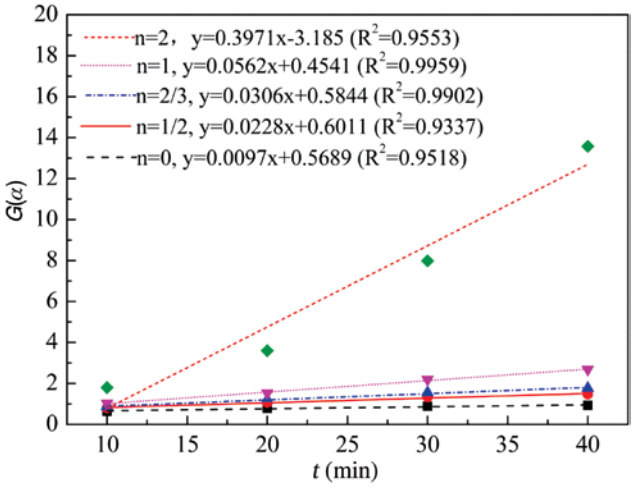

Figure 11: The relationship between $G(\alpha)$ and time at 600°C on n=0, 1/2, 2/3, 1, 2, respectively.

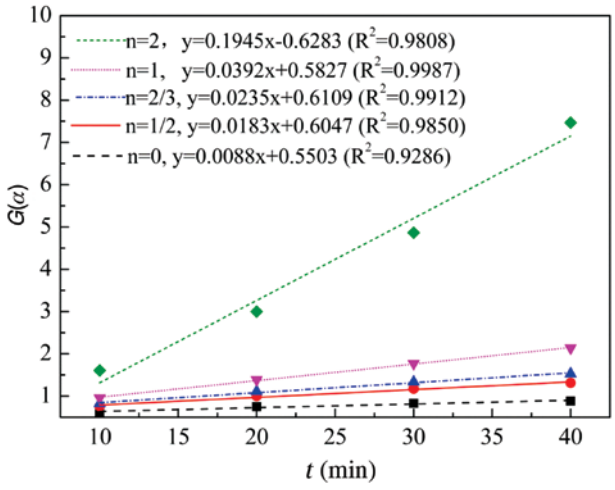

Figure 12: The relationship between $G(\alpha)$ and time at 550°C on n=0, 1/2, 2/3, 1, 2, respectively.

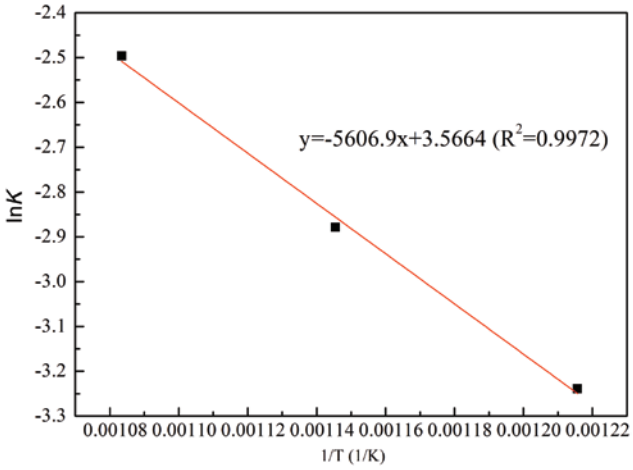

Figure 13: Relationship between ln$K$ and 1/T for the zinc oxide dust.

Table 6: The relationship between mechanism function and time at 600°C.

Reaction order	Fitting line	R^2
0	y=0.0097x+0.5689	0.9518
1/2	y=0.0228x+0.6011	0.9337
2/3	y=0.0306x+0.5844	0.9902
1	y=0.0562x+0.4541	0.9959
2	y=0.3971x-3.185	0.9553

Table 7: The relationship between mechanism function and time at 550°C.

Reaction order	Fitting line	R^2
0	y=0.0088x+0.5503	0.9286
1/2	y=0.0183x+0.6047	0.985
2/3	y=0.0235x+0.6109	0.9912
1	y=0.0392x+0.5827	0.9987
2	y=0.1945x-0.6283	0.9808

Table 8: Relationship between ln$K$ and 1/T.

T (°C)	K	ln$K$	1/T (1/K)
550	0.0392	-3.2391	0.00121567
600	0.0562	-2.8788	0.00114548
650	0.0824	-2.4962	0.00108342

The dependences of the calculated value of ln$K$ versus 1/T are shown in Figure 13, which include the activation energy of zinc oxide dust calculated by the Arrhenius equation.

From Figure 13 can be obtained the linear equation fitting ln$A$=3.5664, then A=35.4, E/R=5606.9, then the activation energy E was 46.6 KJ/mol, which is relatively small, indicating that the volatilization of metal chlorides exists at 550°C~650°C when the diffusion-controlled reaction order n is level 1. The volatile reaction mechanism function $f(\alpha)$ of zinc oxide dust can be expressed as shown in Eq. (13), and the volatile reaction kinetics can be described by Eq. (14):

$$f(\alpha)=1-\alpha \tag{13}$$

$$G(\alpha)=e^{-5606.9/T}\times 35.4t \tag{14}$$

Various kinetic models have been developed for analyzing the solid-state reactions [36–39]. Zhu et al. [40] put forward a process of recovering Ge by chlorinating roasting and the reaction rate is controlled by the diffusion velocity of HCl and $GeCl_4$ in the solid product layer, and the activation energy of 22.236 kJ/mol was determined for the chlorinating roasting reaction, which is smaller than the value observed in this work. In our study, the metal chlorides were rapidly dissociated with increase in temperature by microwave heating, which was so high that the system was controlled by the solid state diffusion. Feng et al. [38] proposed the fluidized roasting reduction technology of low-grade pyrolusite coupling with pretreatment of stone coal; the reduction process is controlled by the interface chemical reaction with an apparent activation energy of 36.397 kJ/mol. When the progressive volatilization reaction of the metal chlorides in oxygen and water is considered, another possible volatilization mechanism is kinetic control by an interface chemical reaction.

As a result, the present work shows that the dechlorination process is possibly controlled by the solid state diffusion and interface chemical reaction with an activation energy of 46.6 kJ/mol.

Based on the above experimental results and analysis, for enhancing the dechlorination from zinc oxide dust by microwave heating, the effect of dechlorination is dependent on the metal chloride at temperatures below 650°C. However, the reaction of the metal chloride combined with oxygen and water is enhanced at temperatures >732°C. Therefore, development-related research on the effect of high temperature water vapor and air for dechlorination in a follow-up study is very important. At the same time, studying a new method of removing chlorine by microwave roasting is of great significance for dealing with different kinds of zinc dust resources, as well as realizing its reuse and comprehensive recovery. Moreover, it also has the potential advantage of energy efficiency in the zinc hydrometallurgy process.

4 Conclusions

1. The loss factors of zinc chloride and lead chloride were higher than those of zinc oxide and lead oxide, respectively, and the dielectric loss of zinc oxide dust was the highest in these substances (zinc oxide dust, ZnO, $ZnCl_2$, PbO and $PbCl_2$). Utilizing the selective heating property of microwaves, the zinc (lead) oxide and impurities (chloride) can be effective segregation.
2. The dechlorination effect of zinc oxide dust by microwave roasting shows some advantages such as high% Cl removed (97.22%), rapid heating (40 min) and low roasting temperature (650°C), which extends a wide industrial prospect.
3. The comparison of X-ray diffraction (XRD) patterns shows that most of $ZnCl_2$(s) and $PbCl_2$(s) in zinc oxide dust has been removed.
4. The volatile kinetics of zinc oxide dust were controlled by the solid state diffusion and interface chemical reaction during the microwave heating, with an activation energy of E=46.6 KJ/mol and the reaction order n is 1 level [32].

Acknowledgments: This work was supported by the National Natural Science Foundation of China (51104073), National Program on Key Basic Research Project of China (2014CB643404), National Basic Research Program of China (2012HB008), Yunnan Provincial Science and Technology Innovation Talents scheme Technological Leading Talent (2013HA002), and the 2014 PhD Newcomer Award in Yunnan Province (1319880207).

References

[1] Jha MK, Kumar V, Singh RJ. *Resour. Conserv. Recycl.* 2001, 33, 1–22.
[2] Dutra AJB, Paiva PRP. *Tavares LM. Miner. Eng.* 2006, 19, 478–485.
[3] Peng N, Peng B, Chai LY, Li M, Wang JM, Yan H, Yuan Y. *Miner. Eng.* 2012, 35, 57–60.
[4] Al-Harahsheh M, Kingman S. *Chem. Eng. Process.* 2007, 46, 883–888.
[5] Lashgari M, Hosseini F. *J. Chem.* 2013, 2013, 1–5.
[6] Güresin N, TopkayaYA. *Hydrometallurgy* 1998, 49, 179–187.
[7] Cinar Sahin F, Derin B, Yücel O. *Scand. J. Metall.* 2000, 29, 224–230.
[8] Lan YZ, Zhao QR, Smith RW. *Miner. Process. Extr. Metall.* 2006, 115, 117–119.
[9] Jiang L, Fu GF, Wang DQ. *Nonferr. Metal.* 2001, 53, 28–31. (In Chinese).
[10] Qiu YY, Zhao YC, Zhang CL, Yi TS. *J. Safety Environ.* 2008, 8, 62–64. (In Chinese).
[11] Mason CRS, Harlamovs JR, Dreisinger DB, Grinbaum B. *US Patent*, Appl. 7037482B2, 2006.
[12] Bodson FJJ. *US Patent*, Appl. 4005174, 1977.
[13] Pickles CA. *Miner. Eng.* 2009, 22, 1102–1111.
[14] Pickles CA. *Miner. Eng.* 2009, 22, 1112–1118.
[15] Nanthakumar B, Pickles CA, Kelebek S. *Miner. Eng.* 2007, 20, 1109–1119.
[16] Prajapat AL, Gogate PR. *Chem. Eng. Process.* 2015, 88, 1–9.
[17] Haque KE. *Int. J. Miner. Process.* 1999, 57, 1–24.
[18] Jin QH. *Beijing: Beijing Science and Technology Press,* 1999, 17–20. (In Chinese).
[19] Guo ZY, Lei T, Li W, Ju SH, Peng JH, Zhang LB. *Chem. Eng. Process.* 2015, 92, 67–73.
[20] Wei YQ, Peng JH, Zhang LB, Ju SH, Xia Y, Zheng Q, Wang YJ. *J. Cent. South Univ.* 2014, 21, 2627–2632.
[21] Patil NG, Rebrov EV, Eränen K, Benaskar F, Meuldijk J, Mikkola JP, Schouten JC. *J. Microwave Power E. E.* 2012, 46, 83–92.
[22] Ma AY, Zhang LB, Peng JH, Chen G, Liu CH, Xia HY, Zuo YG. *J. Microwave Power E.E.* 2014, 48, 25–34.
[23] Leonelli C, Mason TJ. *Chem. Eng. Process.* 2010, 49, 885–900.
[24] Dong SY. *Beijing: Beijing University of Science and Technology Press*, 1991, 327–330. (In Chinese).
[25] Zenki M, Iwadou Y. *Talanta* 2002, 58, 1055–1061.
[26] Peng ZW, Hwang JY, Mouris J, Hutcheon R, Huang XD. *ISIJ Int.* 2010, 50, 1590–1596.
[27] Zeng ZG, Dou CL, Liu WP, Xi XM, Xiao SW. *Min. Metall. Eng.* 2007, 27, 54–56. (In Chinese).
[28] Li RD, Li YL, Wang L, Tian XH, X Ke, Wei LH, Yang TH. *J. Combust. Sci. Technol.* 2010, 16, 30–34. (In Chinese).
[29] Wang CG, Hu XJ, Matsuura H, Tsukihashi F. *ISIJ Int.* 2007, 47, 370–376.
[30] Li RD, Li YL, Wang L, Zhang HJ, Ke X, Wei LH. *J. Combust. Sci. Technol.* 2009, 8, 57–63. (In Chinese).
[31] Zhang YL, Fu ZH, Li SQ, Wang YG, Fu XB. *Chinese J. Nonferr. Metal.* 2011, 21, 450–458. (In Chinese).
[32] Fu YM. *Northeastern University.* 1997, 11–14. (In Chinese).
[33] Şahin FÇ, Derin B, Yücel O. *Scand. J. Metall.* 2000, 29, 224–230.
[34] Taxak M, Krishnamurthy N. *J. Alloys Compd.* 2015, 623, 121–126.

[35] Wu FF, Zhong H, Wang S, Lai SF. *J. Cent. South Univ. Technol.* 2014, 21, 1763–1770.
[36] Chakravortty M, Srikanth S. *Thermochim. Acta* 2000, 362, 25–35.
[37] Tathavadkar VD, Antony MP, Jha A. *Metall. Mater. Trans. B.* 2001, 32, 593–602.
[38] Feng YL, Cai ZL, Li HR, Du ZW, Liu XW. *Int. J. Miner. Metall. Mater.* 2013, 20, 221–227.
[39] Cong J, Yan DH, Li L, Cui JX, Jiang XG, Yu HJ, Wang Q. *Environ. Eng. Sci.* 2015, 32, 425–435.
[40] Zhu GC, Wang JY, Cheng Z, Zhao Y. *Rare Met.* 2008, 27, 238–242.

Bionotes

Aiyuan Ma

Aiyuan Ma started his PhD at Kunming University of Science and Technology, China, where he is currently carrying out research on comprehensive utilization of resources, hydrometallurgy and unconventional metallurgy under the supervision of Professor Jinhui Peng. His main research subject is zinc extraction from the blast furnace dust by the ammonia process.

Xuemei Zheng

Xuemei Zheng started her MSc at the Kunming University of Science and Technology, China, where she is currently carrying out research on metallurgy and chemical engineering under the supervision of Professor Jinhui Peng. Her primary research interests include hydrometallurgy and comprehensive recovery of the secondary zinc resources by ultrasonic metallurgy.

Shixing Wang

Shixing Wang is a senior engineer at Kunming University of Science and Technology. He received a Bachelor's degree in 1999 from Sichuan Normal College, China and a Master's degree in 2002 from Kunming Institute of Precious Metals, China. In 2008, he earned a PhD degree in Xi'an Jiaotong University. His current research interests include nanotechnology, non-ferrous metallurgy and hydrometallurgy.

Jinhui Peng

Jinhui Peng is a PhD supervisor in Kunming University of Science and Technology, and is mainly engaged in microwave heating in the application of metallurgy, chemical engineering and materials science. He has received many awards, among which are the State Technological Invention Award and the Natural Science Award of Kunming province.

Libo Zhang

Libo Zhang is a PhD supervisor in Kunming University of Science and Technology, and is mainly engaged in microwave heating in the application of metallurgy, chemical engineering, material, etc.

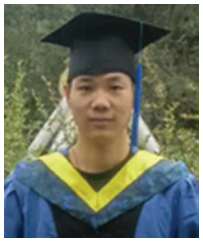

Zhiqiang Li

Zhiqiang Li started his MSc at Kunming University of Science and Technology, China, where he is currently carrying out research on microwave energy application, metallurgy and chemical engineering under the supervision of Professor Libo Zhang. His main research subject is the separation of detrimental impurities from zinc oxide dust.